Research Article ISSN 2832-9384

Journal of Materials and Polymer Science

Dynamics of RBCs and Their Charge Development Due to Laser Beam During The Pre-Ionization Period

Bekalu T. Melaku[1*], Daniel B. Erenso[2]

[1]*Department of Physics, Addis Ababa University.*

[2]*Department of Physics and Astronomy, Middle Tennessee State University.*

***Corresponding author**

Bekalu T. Melaku,
bekalu.tesfaye@eiabc.edu.et
Department of Physics,
Addis Ababa University,
Ethiopia.

Submitted : 17 Apr 2024 ; Published : 24 Jun 2024

Citation: Bekalu T. Melaku & Daniel B. Erenso(2024). Dynamics of RBCs and Their Charge Development Due to Laser Beam During The Pre-Ionization Period , J mate polysci, 4(2):1-13. DOI : https://doi.org/10.47485/2832-9384.1056

Abstract

In this paper it is attempted to have a closer understanding of a cell when it is subjected to a highly focused laser beam giving a special attention to a single ionized cell during its pre-ionization phase. Cells of varying size are subjected to a 1064nm near infrared (NIR) radiation one by one and their trajectory (radial and tangential) towards the center of the trap has been recorded and analyzed. The result showed that the cells gain charge even before being trapped by the trapping center i.e. while they are on their way to the center. As a result, the charged cells have been observed interacting with the electromagnetic field creating a Coulomb force in the direction of polarization. Consequently, the developed charge significantly affected the trajectory of each cell towards the trap center by retarding those cells whose gradient force vector and direction of polarization are in opposite direction while accelerating those cells whose gradient force vectors align to the direction of polarization.

Keywords: laser trapping, gradient force, single-cell ionization, pre-ionization stage, ionization-stage, post-ionization stage.

Introduction

Ever since manipulating micron sized dielectric spherical objects using a near infrared (NIR) laser light had been shown to be possible (Ashkin, 1992), several advancements have been made in the area of biophysics, biotechnology and bio-photonicsby allowing free manipulation of cells (Huisjes et al., 2018), neutral atoms (Phillips, 1998), macromolecules such as DNA strands, and microspheres and their microflows (Ellingsen, 2013).

Major causes that enable manipulation of cells by laser trap (LT) are

- momentum carried by light
- size of cells and their dielectic property when subjected to laser light
- the intensity and gradient of the laser light. Light photons carry momentum related to their wavelength but its effect will be significant only when the wave length is way below the size of the particle it is imparted to (geometric optics regime) which would otherwise fall in the Rayleigh regime and considers the object as a dipole.

The dielectric nature of cells when subjected to laser light keeps the cells from oscillating due to periodic EM field of the laser. This is another significant factor manipulating cells by LT techniques becomes possible. As a result, cells (average diameter 5μm) will move steadily in the direction of the laser propagation (or pointing vector) instead of oscillating at optical frequency(Solomon et al., 2013).These two properties of light and cells will only allow us to push or suspend the cells in one direction, and thus, making manipulation to be one directional. However, manipulation of cells in more than one direction is possible if the laser light has an intensity gradient (Ashkin, 1992), this allows motion of cells in the remaining directions, and hence, trapping possible.

Brief description of applications of laser trapping techniques in researches involving manipulation of RBCs is made here below.

LT and Diabetes

One very important property of RBCs is their property to bind together, i.e. coagulation, which determines the viscosity of blood. This, in turn, plays a significant role in the process of blood circulation throughout our body. Various diseases are caused by luck of improper circulation of RBCs such as stroke and diabetes. In an effort to study this important property of RBCs, i.e. aggregation of RBCs, numerous attempts are made to estimate the binding and disaggregation forces between two RBCs. According to the study made, for example by Priezzhev and Lee (2016), the force for aggregation is significantly greater than that of disaggregation force. In addition, the

values are considerably different for cells taken from diabetes patients illustrating cellular level identification of normal and diabetes mellitus patients. Such hemorheological properties of cells became possible applying LT technique. The basic procedure was that two cells were handled using two infrared laser beams making one of the beams fixed while the other being probe laser beam and measuring the trapping force from the laser power needed to just disaggregate or aggregate the cells(Priezzhev & Lee, 2016; Semeno et al., 2016).

LT and Anemia

Another application of LT is in the determination of physical, mechanical (Solomon et al., 2013; Pellizzaro et al., 2012) and chemical properties (Kelley et al., 2018) of human RBCs. The physical and mechanical properties has been studied by measuring the size of the RBC before and during the laser trap of normal and sickle cell anemia (SCA) patient cells to investigate the relative deformations of the two samples. The study (Solomon et al., 2013) showed that deformation (squeezed size) can be correlated with hemoglobin quantitation giving a clue about the possible identification of sickle cell anemia (SCA) patient from the healthy ones. Furthermore, based on the relaxation time (the time required for the cell to recover to its relaxed size after it was squeezed during ionization for varying laser power), it was possible to get additional information in identifying SCA blood samples.

In addition to methods like high performance liquid chromatography (HPLC) of determining hemoglobin quantitation (Kutlar et al., 1984), another approach to finding the charge and chemical composition of cells was shown to be possible in a recent research (Kelley et al., 2018). The study was conducted by ionizing (trapping) cells at an individual level and letting them ejected out of the laser trap. Analysis of the duration of ionization and scrutinizing the trajectory of ejection revealed significant difference between normal RBCs and those with SCA.

Other similar researches in relation to RBCs manipulation at single cell level with LT techniques are being done. These researches focus on the study of the behavior of RBCs during ionization and the dynamics of the cells after ionization. However, in addition to such studies, investigation of the trajectory of the cells before they are trapped by the laser beam can be potential area of research for, they can give additional information of the RBCs.And, thus, the study of the dynamics of the cell prior to ionization will be the primary focus of this paper.

In the next section, methodologies followed in setting up the LT laboratory and sample preparation of RBCs will be describe briefly.

Materials and Methods

Sample preparation

The biological sample used was human breast carcinoma cells BT20. The BT20 cells were obtained from American Type Culture Collection (ATCC) and grown in the growth media RPMI-1640, supplemented with 10% fetal bovine serum (FBS) and 100 U/mL penicillin/streptomycin. The cells were incubated in a humidified atmosphere with 5% CO_2 at 37°C, and cells with a passage number 5-10 were used for the following assays. The cells were harvested from the culturing vessel by using 1X trypsin-EDTA solution, and re-suspended in the growth media at an intensity of 2×10^4 cells/mL.

Experimental set-up

A single LT experiment basically involves laser source, optical instruments that control the laser light and refractive lenses of various indices in addition to a high speed camera. Laser light from the source is permitted to pass through successive optical units that polarize, expand, reflect, magnify and finally focus the light on the stage. In effect, the micron-sized objects laid on the stage were suspended on the focal plane and gravitated towards the focused light. Simplified options in developing laser trapping laboratory are available, even for undergraduate level at an affordable price (Wieman et al., 1995; Bechhoefera & Scott, 2022; Smith et al., 1999).

The laboratory and the design for our experimental set-up is the same as it had been used by Kelley et al. (2016), Pellizzaro et al. (2012) and is shown in Fig. 1. Following the design (from top left) we have a linearly polarized infrared diode laser source (LS) producing 8 watts at 1064nm with a beam size of 4mm. The power was controlled by a λ/2-wave plate (W) and polarizer (P) combination. In order to ensure the position of the trap on the focal plane of the microscope we use a series of converging and diverging lenses beginning with the beam expander (BE) and through lenses (L1-4). The mirrors (M1-4) are used to align and direct the laser beam through a port of an inverted microscope (IX 71-Olympus). A perfectly aligned beam would then be redirected for a normal incidence angle at the center of the back of an objective lens (OL) using a dichroic mirror (DM) positioned at 45° inside the microscope. The OL has a 100X magnification and a 1.25 numerical aperture (Edmund Optics). The microscope is equipped with piezo-driven (NS) stage to house and better manipulate the microscope slide and a digital camera (CCD) to take a live 2D bright-field contrast image of the sample in the slide using 30mW halogen lamp (HL). Both the piezo-driven stage and the digital camera are interfaced with a computer (PC).

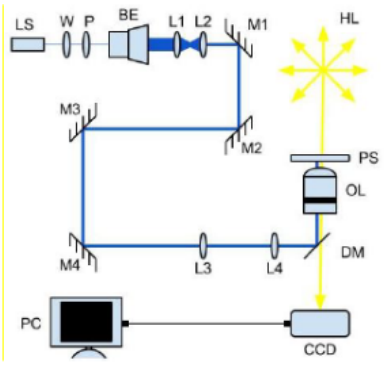

Figure 1: The experimental set-up for the single laser trap (Solomon et al., 2013; Kelley et al., 2016).

Image Processing

Having completed the process of capturing images of the cell from the CCD camera (which has a capacity of taking over 20 pictures per second), image analysis has been performed using image pro-plus software. With this software, huge numbers of images were analyzedas inthe next important procedures.

First, the images were merged to sequence files so that they can be analyzed as a video file. Next to this, various filtering tools which were relevant to properly identify the cell and take reasonable measurements from the images has been used. For better estimation of the cellular area, the Sobel edge filtering tool in the Process toolbar was selected. Sobel filter (go to Filters>Edge tab>Filters frame >Sobel option button) enhances the principal edges of the cell. Another important tool that gives the images a clearer view is the Sharpen tool (go to Filters>Enhancement>Sharpen-Options frame) the value 7x7 is selected and Passes 1 and strength 10 are set. In addition, automatic dark objects (got to Count/size dialogue box > Intensity Range Selection frame box > Automatic Dark Objects) were selected for correct area representation or better estimate of cell size. To avoid clustered cells from being considered as one cell, Watershade Split tool (found in the menu list of Count/Size dialogue box) or (Tracking options menu > Objects in tracks frame box > Auto split objects Checkbox > Use watershade split Checkbox) has been used thus clustered cells were separated and measurements of each cell became possible. After using all these filtering mechanisms, the software identified unrealistic shapes as a cell. This was circumvented by setting additional criteria such as providing ranges of reasonable values for certain measurements. The data in this paper has been obtained by setting reasonable ranges of values for area (between 150 to 2500 pixel squares) and roundness (between 0.2 to 3.2). (Go to Measurements dialogue box in the Measure menu found in the Count/Size dialogue box).

Once the filtering was done and the cells within a reasonable size were identified, the areas and positions of every cell in every frame were obtained using the Track Objects command (Measure> Track Objects) after setting the various tracking options including the frame interval. All the observations and analyses in the following sections have been made based on these measured data.

Phases of Cell Trapping

We can subdivide the trapping stages of RBCs in to before, during and after ionization since they have entirely different dynamical behavior and can be studied independently. For example, trajectory of atypical cell during its three phases of trapping is shown in Fig. 2. As can be seen, the first phase extends from t=0 to t=8.3sec and the second phase from 8.3sec to 12sec and the last phase for t>12sec.

At the beginning of the first phase, the cell shows lesser slope and the slope increases as it approaches its trapping time and becomes sharp just before it is being trapped. During ionization phase, the cell stays at its position with jittering of small distance. Possible cause of jittering, apart from the error due to capturing the actual position of the cell, is vibratory motions of the cell and its contents due to some rapturing of the cell membrane.

The last phase of the cell, post ionization stage, is characterized by its higher slope and short duration. The large slope informs the very high speed the cell attains as it ejects out of the trap. Usually, after ejection, the cell cannot be capture well due to its high speed of ejection and disappearance of cell from the focal plane. Consequently, only few points can be recorded.

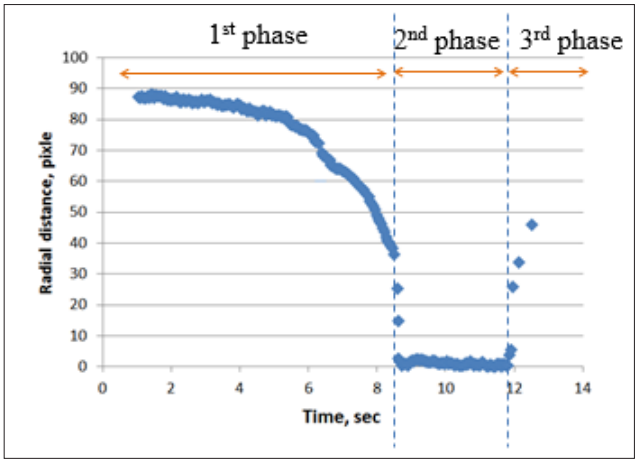

Figure 2: Cell Laser Trapping Phases

Another important thing we can get from the recorded graph is the information the density of the data points convey. The denser the data points implies the slower the velocity of the cell whereas sparse data points tell the very high speed the cell has during that time. The reason is that the CCD camera has been set to have a constant capturing rate (approx. 20 pictures/sec) and, therefore, fast moving objects can be captured less frequently.

Data Analysis

The measured and recorded experimental data for the coordinates of the cell were analyzed and radial and angular positions of the cell with respect to time as measured from the trap center were generated. Fig. 3shows the radial distance vector $(\vec{r})$ is directed towards the trap center which was obtained from the coordinates of the cell and that of the trap center while polarization vector $(\vec{n})$, was calculated from the positions of the cell after ejection and the position of the trap center. Obviously, the radial and angular vectors are time varying vectors unlike the polarization vector.

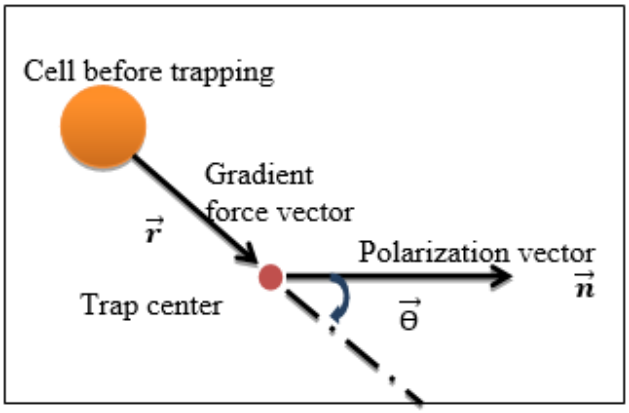

Figure 3: Vectorial Representation of Laser Polarization and Gradient Force

The video file created after merging the successive images captured by the CCD camera made studying the dynamics of the cell easier. Accordingly, the essential observations were noted.Pre-ionization trajectory of cells (path made towards the laser before being trapped) showed fundamental similarity:

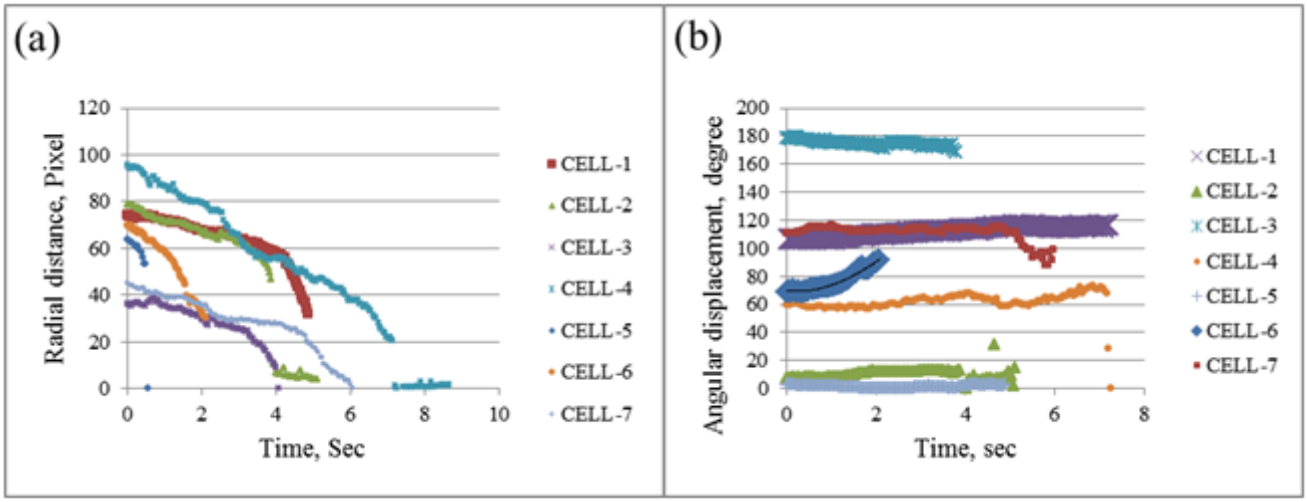

Figure 4: For seven sample cells, the time variation of:
(a) radial position in units of pixel (b) angular position in units of degree fundamental similarity:

- Cells which were far away from the laser center, started moving slowly towards the center;
- While approaching towards the center, the velocity of the cells suddenly changed considerably after a certain radial distance;
- With such high velocity, the cells travelled until being absorbed by the laser beam where they had been ionized for some time and ejected out from the trap center. Despite these similarities, however, there werevisible differences in the pre-ionization trajectories of these cells.
- The critical radial distance (at which the radial velocity abruptly changed) varied for various cells;
- The velocities before and after this critical distance also varied from cell to cell;
- Cells that were located on the opposite side from the direction of ejection (with respect to the trapping center) were attracted more and faster than those cells that were located in the direction of ejection.

Mathematical Modeling

Expected force on the cell before, during and after ionization by the laser had been described as (9) (14):

$$m\frac{d^2r}{dt^2} = qE_0e^{-(r/w_o)^2} - \beta\frac{dr}{dt} + \alpha\nabla\left(E_0e^{(ikr)}e^{-(r/w_o)^2}\right) \quad (1)$$

This can, however, be described in a vector form as:

$$m\frac{d^2\vec{r}}{dt^2} = qE_0e^{-(r/w_o)^2}\hat{n} - \beta\frac{d\vec{r}}{dt} + \alpha\vec{\nabla}\left(E_0e^{(ikr)}e^{-(r/w_o)^2}\right)$$
$$m\frac{d^2\vec{r}}{dt^2} = qE_0e^{-(r/w_o)^2}\hat{n} - \beta\frac{d\vec{r}}{dt} + \alpha E_0\left(ik - \frac{2r}{w_o^2}\right)e^{\left(ikr-(\frac{r}{w_o})^2\right)}\hat{r} \quad (2)$$

Here, the direction of polarization, $\hat{n}$, the velocity and acceleration of the cell are decomposed into their radial and tangential components as:

$$\hat{n} = n(r)\hat{r} + n(\theta)\hat{\theta} \qquad \text{where } n(r) = -\hat{n}*\hat{r} \text{ and } n(\theta) = \sin\left(cos^{-1}(-\hat{n}*\hat{r})\right)$$
$$\frac{d\vec{r}}{dt} = v(r)\hat{r} + v(\theta)\hat{\theta} \qquad \frac{d^2\vec{r}}{dt^2} = a(r)\hat{r} + a(\theta)\hat{\theta}$$
$$m\frac{d^2\vec{r}}{dt^2} = F(\theta)\hat{\theta} + F(r)\hat{r} = \left\{qE_0e^{-(r/w_o)^2}n(\theta) + \beta v(\theta)\right\}\hat{\theta} + \left\{qE_0e^{-(r/w_o)^2}n(r) + \beta v(r) + \alpha E_0\left(ik - \frac{2r}{w_o^2}\right)e^{\left(ikr-(\frac{r}{w_o})^2\right)}\right\}\hat{r} \quad (3)$$

Since it is possible to express left-hand-side as:

$$m\frac{d^2\vec{r}}{dt^2} = m\left(r\ddot{\theta} + 2\dot{r}\dot{\theta}\right)\hat{\theta} + m\left(\ddot{r} - r\dot{\theta}^2\right)\hat{r} = F(\theta)\hat{\theta} + F(r)\hat{r}$$

Then,

$$F(\theta) = m\left(r\ddot{\theta} + 2\dot{r}\dot{\theta}\right);\ F(r) = m\left(\ddot{r} - r\dot{\theta}^2\right) \quad (4)$$

Therefore, from Eq. (3) and Eq.(4)

$$q = \{m(r\ddot{\theta} + 2\dot{r}\dot{\theta}) - \beta r\dot{\theta}\}/\{E_0 e^{-(r/w_o)^2}\, n(\theta)\} \quad (5)$$

$$m\left(\ddot{r} - r\dot{\theta}^2\right) = qE_0 e^{-(r/w_0)^2} e^{-(r/w_0)^2} n(r) + \beta v(r) + \alpha E_0 \left(ik - \frac{2r}{w_0^2}\right) e^{\left(ikr - \left(\frac{r}{w_0}\right)^2\right)} \quad (6)$$

Eq. (5) can be solved numerically if the position of the cell at every instant of time is recorded and direction of ejection is known. However, as can be seen from Fig. 4, both graphs showing the radial and angular positions of the cell are not smooth which is characteristic to any experimental data. For this particular case, among other possible reasons for the abrupt change in position of the cells, low camera resolution and imperfection in processing the images of the cell can be attributed to the non-smooth cell trajectory. This will make finding the first and second derivative of the radial and angular positions (i.e. radial and angular velocities) at every point impossible. This in turn jeopardizes finding the developed charge that would be obtained by solving Eq. (5).

The numerical challenge has been overcome by fitting the radial position data by two second order polynomials and the angular position data by sixth-order polynomial to a reasonable accuracy. This way, the radial and angular velocities were obtained at ease by differentiating the fitted polynomials. See below the experimental data for the radial and angular positions of Cell#1 and the respective fitted graphs. Fig. 5 (a), (b) and (c) show the fitting of the radial position data in two second-order polynomials (one up to19th second and the other after the 19th second) with more than 0.95 R2 values whereas Fig. 5(d)the fitting of the angular position data in a sixth order polynomial with more than 0.9 R^2.

Pre-ionization charge development for seven cells is shown in Fig. 6 (a) and Fig. 6 (b) is the same as (a) but Cell-2 is removed for a closer look of the other cells due to scaling reason. It can be perceived that the charge development is oscillatory in nature. Moreover, the initial charge shows randomness while the trend of the charge as it gets to the trapping moment sharply changes to zero.

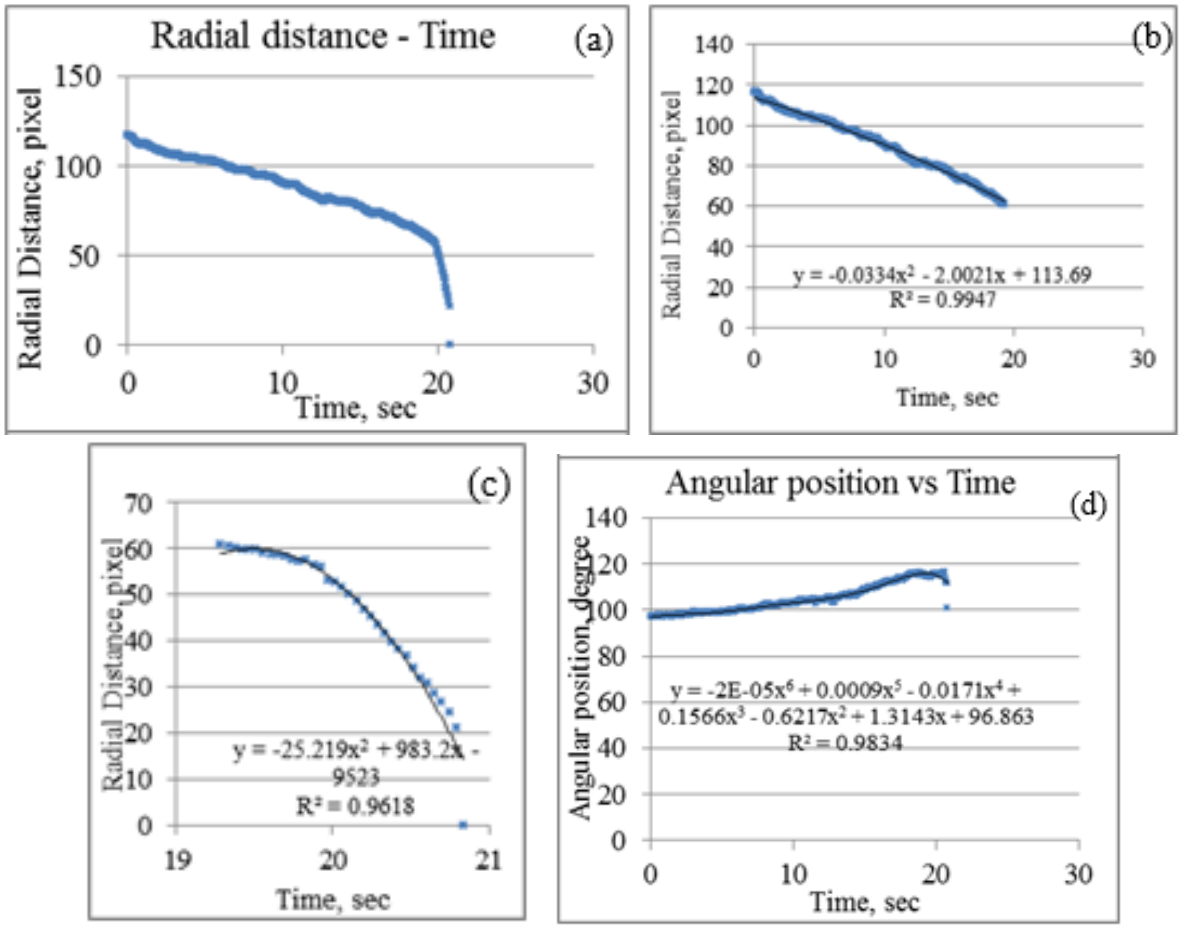

Figure 5 : Curve-fitting of radial and angular positions of the cell
(a) Unfitted radial position curve
(b) 2nd order fit for the gentled slope part of the radial position curve
(c) 2nd order fit for the steeper part of the radial position curve
(d) 6th order fit for the angular position curve

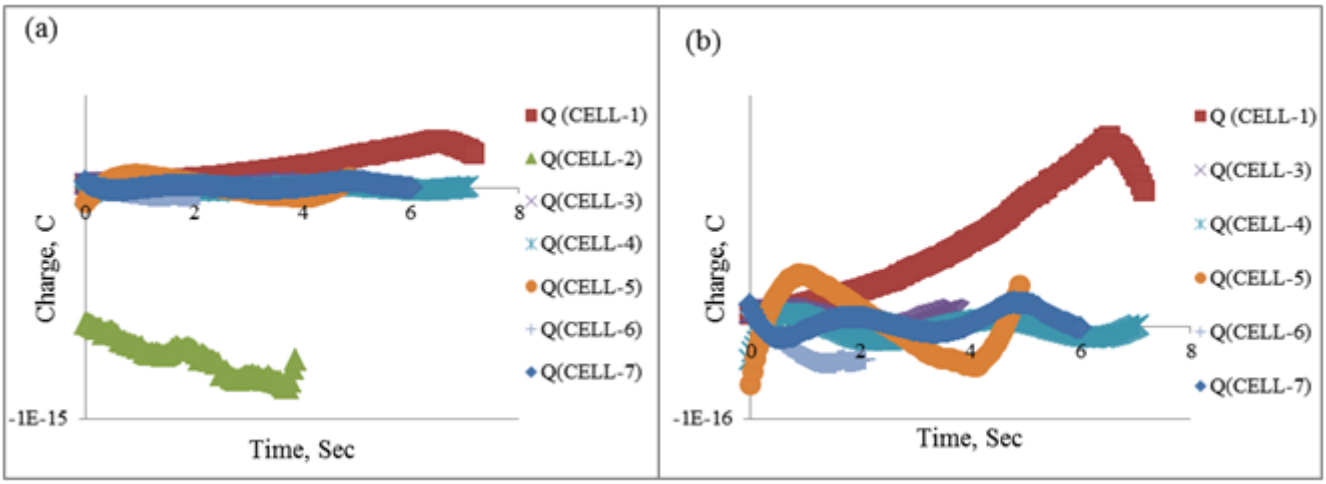

Figure 6: Pre-ionization charge development

It is noteworthy that the charge development and the acceleration of the cell towards the trap center are highly sensitive to the θ component of polarization vector, i.e. $n(\theta)$.

Conclusion

This suggests the possibility that cells are pushed towards the direction of polarization (time-independentvectordirected away from the trap center) in addition to the trapping force (whose direction vector is time varying and heading always towards the center of the trap). The two forces will, thus, have additive effect on the cells whenever the trapping force vector has a component aligned towards the direction of ejection (Fig. 7(a)) whereas subtractive effect otherwise (Fig. 7(b)).

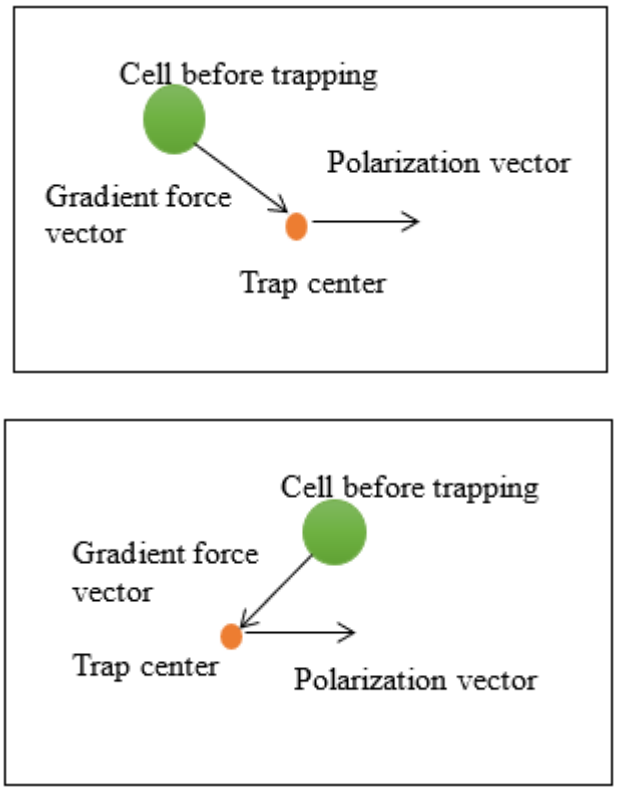

Figure 7: Significant force vectors (gradient and Coulomb) acting on a cell when the vectors have
(a) additive components (b) subtractive components

References

1. Ashkin, A. (1992). Forces of a single-beam gradient laser trap on a dielectric sphere in the ray optics regime. *Biophysical Society, 61*(2), 569-582. DOI: 10.1016/S0006-3495(92)81860-X
2. Huisjes, R., Bogdanova, A., van Solinge, W. W., Schiffelers, R. M., Kaestner, L., & van Wijk, R. (2018) .Squeezing for life – Properties of red blood cell deformability. *Front Physiol*, 9, 656. DOI: 10.3389/fphys.2018.00656
3. Phillips, W. D. (1998). Laser cooling and trapping of neutral atoms. *Reviews of Modern Physics, 70*(3), 721-741. Retrieved from https://cdn.journals.aps.org/files/RevModPhys.70.721.pdf
4. Ellingsen, S. A. (2013). Theory of microdroplet and microbubble deformation by Gaussian laser beam. *Journal of the Optical Society of America, 30*(6). DOI: 10.1364/JOSAB.30.001694
5. Solomon, R., Cooper, J., Aguilar, E., Welker, G., Pennycuf, C., Scott, D. & Flanagan, B. (2013). Physical and mechanical properties of the human red blood cells with different hemoglobin types. Proceedings of the National Conference On Undergraduate Research (NCUR) 2013 University of Wisconsin, La Crosse, WI April 11-13,pp. 532-540. Retrieved from https://libjournals.unca.edu/ncur/wp-content/uploads/2021/10/450-Aguilar.pdf
6. Priezzhev, A. & Lee, K. (2016). Potentialities of laser trapping and manipulation of blood cells in hemorheologic research. *Clin Hemorheol Microcirc, 64*(4), 587-592. DOI: 10.3233/CH-168030
7. Semeno, A., Kisung, L., Lugovtsov, A. E., & Priezzhev, A. (2016). Laser trapping for red blood cells interaction force measurement in aggregation and disaggregation. *Advanced Laser Technologies* (ALT'16).
8. Pellizzaro, A., Welker, G., Scott, D., Solomon, R., Cooper, J. P., Farone, A. L., Farone, M., Mushi, R., Aguinaga, M. del P., & Erenso, D. (2012). Direct laser trapping for measuring the behavior of transfused erythrocytes in a sickle cell anemia patient. *Biomedical Optics Express 3*(9), 2190-9. DOI: 10.1364/BOE.3.002190

9. Kelley, M., Cooper, J., Devito, D., Mushi, R., Aguinaga, M. del P., & Erenso, D. B. (2018). Laser trap ionization for identification of human erythrocytes with variable hemoglobin quantitation. *J Biomed Opt, 23*(5), 1-10. DOI: 10.1117/1.JBO.23.5.055005
10. Kutlar, A., Kutlar, F., Wilson, J. B., Headlee, M. G., & Huisman, T. H. (1984).Quantitation of hemoglobin components by high-performance cation-exchange liquid chromatography: its use in diagnosis and in the assessment of cellular distribution of hemoglobin variants. *Am J Hematol, 17*(1), 39-53. DOI: 10.1002/ajh.2830170106
11. Wieman, C. E., Flowers, G., & Gilbert, S. (1995). Inexpensive laser cooling and trapping experiment for undergraduate laboratories. *American Association of Physics Teachers, 63*(4), 317-330. DOI: 10.1119/1.18072.
12. Bechhoefera, J. & Scott, W. (2002). Faster, cheaper, safer optical tweezers for the undergraduate laboratory. *American Association of Physics, 70*(4), 393-400. DOI: 10.1119/1.1445403
13. Smith, S. P., Bhalotra, S. R., Brody, A. L., Brown, B. L., Boyda, E. K., & Prentiss, M. (1999). Inexpensive optical tweezers for undergraduate laboratories. *American Association of Physics Teachers*, 67, 26-35. DOI: https://doi.org/10.1119/1.19187
14. Kelley, M., Gao, Y., & Erenso, D. (2016). Single cell ionization by a laser trap: a preliminary study in measuring radiation dose and charge in BT20 breast carcinoma cells. *Biomed Opt Express, 7*(9), 3438–3448. DOI: 10.1364/BOE.7.003438